

RESEARCH

Open Access



# High-content imaging analyses of $\gamma$ H2AX-foci and micronuclei in TK6 cells elucidated genotoxicity of chemicals and their clastogenic/aneugenic mode of action

Akira Takeiri<sup>\*</sup> , Kaori Matsuzaki, Shigeki Motoyama, Mariko Yano, Asako Harada, Chiaki Katoh, Kenji Tanaka and Masayuki Mishima

## Abstract

**Background:** The in vitro micronucleus (MN) test is an important component of a genotoxicity test battery that evaluates chemicals. Although the standard method of manually scoring micronucleated (MNed) cells by microscope is a reliable and standard method, it is laborious and time-consuming. A high-throughput assay system for detecting MN cells automatically has long been desired in the fields of pharmaceutical development or environmental risk monitoring. Although the MN test per se cannot clarify whether the mode of MN induction is aneugenic or clastogenic, this clarification may well be made possible by combining the MN test with an evaluation of  $\gamma$ H2AX, a sensitive marker of DNA double strand breaks (DSB). In the present study, we aimed to establish a high-content (HC) imaging assay that automatically detects micronuclei (MNi) and simultaneously measures  $\gamma$ H2AX foci in human lymphoblastoid TK6 cells.

**Results:** TK6 cells were fixed on the bottom of each well in 96-well plates hypotonically, which spreads the cells thinly to detach MNi from the primary nuclei. Then, the number of MNi and immunocytochemically-stained  $\gamma$ H2AX foci were measured using an imaging analyzer. The system correctly judged 4 non-genotoxins and 13 genotoxins, which included 9 clastogens and 4 aneugens representing various genotoxic mechanisms, such as DNA alkylation, cross-linking, topoisomerase inhibition, and microtubule disruption. Furthermore, all the clastogens induced both  $\gamma$ H2AX foci and MNi, while the aneugens induced only MNi, not  $\gamma$ H2AX foci; therefore, the HC imaging assay clearly discriminated the aneugens from the clastogens. Additionally, the test system could feasibly analyze cell cycle, to add information about a chemical's mode of action.

**Conclusions:** A HC imaging assay to detect  $\gamma$ H2AX foci and MNi in TK6 cells was established, and the assay provided information on the aneugenic/clastogenic mode of action.

**Keywords:** High content, Genotoxicity, Screening,  $\gamma$ H2AX, Micronucleus, TK6

\* Correspondence: [takeiriakr@chugai-pharm.co.jp](mailto:takeiriakr@chugai-pharm.co.jp)  
Fuji Gotemba Research Laboratories, Chugai Pharmaceutical Co., Ltd., 1-135  
Komakado, Gotemba, Shizuoka 412-8513, Japan



## Introduction

The in vitro micronucleus (MN) test is an important component of a genotoxicity test battery [1]. Although manual scoring by microscope is a reliable and standard method used so far to detect micronucleated (MNed) cells, the method is laborious and time-consuming. In pharmaceutical development, a few promising chemicals need to be efficiently selected from a huge number of candidates in a chemical bank. Moreover, to monitor environmental risk, the genotoxicity of the growing number of chemicals in use should be evaluated efficiently to assess the risk for humans. Therefore, high-throughput assay systems that detect MNed cells automatically have become increasingly desired.

A MN is induced by direct DNA damage (clastogenicity) or by retardation of chromosome segregation (aneugenicity). Revealing the clastogenic or aneugenic mode of action (MoA) is important, especially in pharmaceutical development, which needs to define a threshold of genotoxicity [2]. In general, there is no genotoxicity threshold for clastogens, because direct interaction between a chemical and DNA cannot be ruled out even at very low exposure levels. On the other hand, the target molecules of aneugens are not DNA but components of the mitotic apparatus, such as spindle fibers, in which aneugens interrupt polymerization or depolymerization of tubulins. Therefore, DNA per se is not damaged by aneugens, and abnormal chromosome segregations do not occur at a concentration less than that at which the agent interrupts the functions of the mitotic apparatus. Consequently, if the MoA is taken into account, it is acceptable to set a threshold for aneugens [3]. It is especially important to elucidate an aneugenic MoA at an early stage of pharmaceutical development, because this can avoid eliminating promising candidates on which sufficient safety margins could be set. Moreover, the advance warning of the MoA would be helpful for designing the non-clinical genotoxicity studies used in the late stage of drug development [4]; for instance, using centromeric fluorescence in situ hybridization (FISH) analyses in MN tests under GLP.

Since MN tests alone cannot discriminate aneugens from clastogens, they are usually employed in combination with immunostaining of the kinetochore or FISH analysis of the centromere to discriminate aneugens from clastogens [3, 5]. However, these techniques are not suitable for screening purposes because they are laborious and time consuming.

$\gamma$ H2AX, a phosphorylated form at serine 139 of the histone protein H2AX, was found to be an important component of DNA damage response, especially in sensing and repairing DNA double strand breaks (DSB) [6].  $\gamma$ H2AX is a binding interface of a DSB-repair complex and is amplified to more than 2 M base pairs in the chromatin region around a DSB locus, which then forms

a microscopically visible focus. The  $\gamma$ H2AX focus is considered to be a surrogate marker for a wide range of DNA damage because  $\gamma$ H2AX foci are induced not only by DSB (e.g. by ionizing radiation) but also by DNA single-strand breaks (SSB) after treatment with UV irradiation, topoisomerase inhibitors, and reactive oxygen species [6, 7]. The combination of MN test and  $\gamma$ H2AX detection on a high-throughput platform will make it possible to discriminate aneugens from clastogens in the early screening stages because it was reported that aneugens do not form  $\gamma$ H2AX foci [2] whereas clastogens do. Furthermore, imaging analysis makes it possible to morphologically discriminate  $\gamma$ H2AX foci from pan-nucleic  $\gamma$ H2AX staining, which is believed to be induced by non-genotoxic events, such as apoptosis [8, 9]. Thus, imaging analysis of  $\gamma$ H2AX foci would be an optimal method to specifically evaluate genotoxic events.

Rodent-derived cell lines such as CHL [10] or CHO [11] have been used to evaluate genotoxicity in imaging-based high-throughput systems. However, the predisposition of these cell lines to induce false-positive results more frequently than human-derived cell lines has been raised as a disadvantage. In contrast, the human lymphoblastoid cell line TK6 is noted for its low rate of false positives [12]. Results of genotoxicity tests in TK6 showed the best correlation with those of human lymphocytes, probably because the cell line retains intact p53 [13]. In spite of this advantage, TK6 cells have not been used for imaging-based high-throughput systems because it is difficult to fix non-adherent cells on the bottom of assay plates for imaging analysis.

In the present study, we have established a high-content (HC) imaging assay that detects micronuclei (MNi) in TK6 cells automatically and simultaneously measures  $\gamma$ H2AX foci. Four non-genotoxins, 9 clastogens, and 4 aneugens were subjected to the assay system to evaluate MNi,  $\gamma$ H2AX foci, and cell cycle arrest using an imaging cytometer, In Cell Analyzer 6000. Lastly, the advantages of the test system for evaluating genotoxicity for screening purposes is discussed.

## Materials and methods

### Chemicals

The test chemicals, the vendors, and the CAS Nos. are enumerated in Table 1. The non-genotoxins were sodium dodecyl sulfate (SDS), sodium chloride (NaCl), D-mannitol (D-Man), and nalidixic acid (NA). The clastogens were methyl methanesulfonate (MMS), *N*-ethyl-*N*-nitrosourea (ENU), mitomycin C (MMC), cis-diamminedichloroplatinum (II) (cisplatin, CDDP), irinotecan (CPT-11, CPT), etoposide (ETP), benzo[*a*]pyrene (BaP), cyclophosphamide (CP), and 2-Amino-1-methyl-6-phenylimidazo[4,5-*b*]pyridine hydrochloride (PhIP). The aneugens were colchicine (COL), vinblastine sulfate salt

**Table 1** Test chemicals used in the present study

| Class          | Chemicals  | Abbreviations | CAS No.     | Venders                                      | Major mode of genotoxicity                                |
|----------------|--|---------------|-------------|--|---|
| Non-genotoxins | Sodium dodecyl sulfate   | SDS           | 151-21-3    | Sigma-Aldrich, St. Louis, MO, USA            | -   |
|                | Sodium chloride  | NaCl          | 7647-14-5   | Wako Pure Chemical Corporation, Osaka, Japan | -   |
|                | D-Mannitol   | D-Man         | 69-65-8     | Sigma-Aldrich                                | -   |
|                | Nalidixic acid   | NA            | 389-08-2    | Sigma-Aldrich                                | -   |
| Clastogens     | Methyl methanesulfonate  | MMS           | 66-27-3     | Sigma-Aldrich                                | Guanine N7 alkylation                                     |
|                | <i>N</i> -ethyl- <i>N</i> -nitrosourea                                 | ENU           | 759-73-9    | Sigma-Aldrich                                | Guanine O <sup>6</sup> alkylation                         |
|                | Mitomycin C  | MMC           | 50-07-7     | Kyowa Hakko Kirin, Tokyo, Japan              | Cross-linking   |
|                | Cisplatin  | CDDP          | 15663-27-1  | Sigma-Aldrich                                | Cross-linking   |
|                | Irinotecan   | CPT           | 100286-90-6 | Sawai Pharmaceutical, Osaka, Japan           | Topo I inhibitor  |
|                | Etoposide  | ETP           | 33419-42-0  | Sigma-Aldrich                                | Topo II inhibitor   |
|                | Banzo[ <i>a</i> ]pyrene  | BaP           | 50-32-8     | Sigma-Aldrich                                | Guanine N <sup>2</sup> alkylation by metabolic activation |
|                | Cyclophosphamide   | CP            | 6055-19-2   | Sigma-Aldrich                                | Guanine N7 alkylation by metabolic activation             |
| Aneugens       | 2-Amino-1-methyl-6-phenylimidazo[4,5- <i>b</i> ]pyridine hydrochloride | PhIP          | 105650-23-5 | Wako Pure Chemical Corporation               | Guanine C8 alkylation by metabolic activation             |
|                | Colchicine   | COL           | 64-86-8     | Sigma-Aldrich                                | Microtubule-disruption                                    |
|                | Vinblastine sulfate salt   | VBS           | 143-67-9    | Sigma-Aldrich                                | Microtubule-disruption                                    |
|                | Griseofulvin   | GF            | 126-07-8    | Sigma-Aldrich                                | Microtubule-disruption                                    |
|                | Paclitaxel   | PT            | 33069-62-4  | Sigma-Aldrich                                | Microtubule-disruption                                    |

(VBS), griseofulvin (GF), and paclitaxel (PT). SDS, MMC, CDDP, CPT, and CP were dissolved in sterile distilled water. NaCl and D-Man were dissolved in the culture medium, RPMI-1640 (Nacalai Tesque, Kyoto, Japan) supplemented with 10% fetal bovine serum (FBS, Invitrogen, Carlsbad, CA, USA), 1 mmol/L of sodium pyruvate (Invitrogen), 100 units/mL of penicillin-streptomycin (Invitrogen) and 10 mmol/L of 4-(2-hydroxyethyl)-1-piperazineethanesulfonic acid (HEPES, Invitrogen). MMS, ENU, ETP, BaP, PhIP, COL, GF, and PT were dissolved in dimethyl sulfoxide (DMSO). NA was suspended in DMSO.

### Cells

Human lymphoblastoid TK6 cells were obtained from the American Type Culture Collection (ATCC, Manassas, VA, USA). Cells were cultured in the culture medium at 37 °C in a humidified atmosphere with 5% CO<sub>2</sub>. The doubling time of the cells was approximately 14 h and the modal chromosome number was 47. When treatment was for 24 h without metabolic activation of

S9 mix, a cell suspension was prepared at  $5.3 \times 10^4$  cells/mL in fresh culture medium and seeded into 96-well flat-bottomed plates at  $8 \times 10^3$  cells/well (150  $\mu$ L/well) immediately before the chemical treatment. When treatment was for 3 h with S9 mix followed by a 21-h recovery period (for MN detection), a cell suspension was prepared in the culture medium supplemented with 22% of S9 mix at the same cell density as described above. When treatment was for 4 h with S9 mix (for  $\gamma$ H2AX focus detection), the cell suspension was prepared at  $2.13 \times 10^5$  cells/mL in the culture medium supplemented with 22% of S9 mix and seeded into 96-well flat-bottomed plates at  $3.2 \times 10^4$  cells/well (150  $\mu$ L/well). The S9 mix was prepared by mixing cofactor solution with S9 so that S9 was 12% of the S9 mix solution. The S9 fraction (Wako Pure Chemical Corporation) was derived from the liver of male Sprague-Dawley rats treated with enzyme-inducing agents, phenobarbital and 5, 6-benzoflavone. One milliliter of the cofactor solution consisted of 5.3 mg  $\beta$ -NADP<sup>+</sup>, 2.3 mg glucose-6-phosphate,

0.11 mL of 0.08 mmol/L  $MgCl_2$ , 0.11 mL of 0.6 mol/L sodium phosphate buffer (pH 7.2), and 0.77 mL of the culture medium. After 50  $\mu$ L of test chemical solution/suspension was added to 150  $\mu$ L of the cell suspensions in each well, the final concentration of S9 was approximately 2% ( $22\% \times 12\% \times 150/200 \mu$ L).

#### Treatment with chemicals

Each solution or suspension of the chemical was prepared at a concentration 100-fold higher than the final maximum concentration. The maximum concentrations were selected so that around 50% of relative cell counts (RCC) or relative increase in cell count (RICC) were obtained. Then, the solutions were diluted with culture medium to a concentration 4-fold higher than each final maximum concentration. The resulting solutions/suspensions were serially diluted at a ratio of 1.5 or 1.78 with culture medium to prepare 15 serial concentrations for each chemical. The dilution was conducted in 96-well round-bottomed plates. A 50- $\mu$ L aliquot of each solution/suspension was added to each well, in which cells had been delivered at the levels of density described in the former section, and mixed by pipetting briefly several times. The cells treated with each chemical were cultured at 37 °C in a humidified atmosphere with 5%  $CO_2$  for 24 h (without S9 mix), 4 h (with S9 mix to measure  $\gamma$ H2AX foci), or 3 h (with S9 mix to detect MNed cells). To detect MNed cells, the medium was removed gently after the 3 h treatment with S9 mix so that approximately 50  $\mu$ L remained, in order to avoid losing any cells. The cells were washed with 150  $\mu$ L/well of fresh medium by a gentle pipetting and centrifugation (200 $\times$ g for 5 min at room temperature). After the removal of the medium, 150  $\mu$ L/well of fresh medium was added and the cells were cultured for 21 h.

#### Preparation of fixative

A 4% paraformaldehyde/potassium chloride hypotonic fixative (4% PFA/KCl) was prepared as follows. Eight grams of paraformaldehyde (PFA) was added to 160 mL of ultrapure water that was stirred and heated to 58 °C in a water bath. The PFA was dissolved by adding approximately 80  $\mu$ L of 1 mol/L NaOH and stirring for up to 30 min at 58 °C. After adding 1.12 g of KCl (final concentration 0.075 mol/L), the solution was cooled on ice and adjusted to pH 7.4 by adding several drops of 1 mol/L HCl. The volume was adjusted to 200 mL with ultrapure water and stored at 4 °C for up to 2 weeks. The 4% PFA/KCl was diluted with 0.075 mol/L KCl to prepare a 1% PFA/KCl solution immediately before use.

#### Fixation of cells on 96-well plates

After the treatment with chemicals, each 96-well plate was centrifuged at 200 $\times$ g for 5 min at room temperature.

Most of the culture medium in each well was removed, leaving approximately 50  $\mu$ L in order not to lose any cells from the aspiration. Then 200  $\mu$ L of phosphate buffered saline (PBS) was added to each well and the plate was shaken for 10 s. These steps (from the removal of culture medium to the shaking) were conducted automatically with a plate washer (Bio-Washer 405RS, DS Pharma Biomedical, Osaka, Japan) under a programmed protocol. The centrifuge and washing was repeated 3 times. Then the cell suspension was transferred to a 96-well imaging plate (Corning 3842 Poly-D-Lysin Coat, Corning Inc., Corning, NY, USA) and centrifuged at 200 $\times$ g for 5 min at room temperature, with the acceleration and deceleration rate set at minimum.

After removing all besides 50  $\mu$ L of the supernatant in each well, 200  $\mu$ L/well of 1% PFA/KCl was added gently, and the plate was left for 1 h at room temperature. The fixative was removed in the same manner as in the former step, and 200  $\mu$ L/well of PBS containing 10% FBS was added and the plates were left for 15 min at room temperature (this FBS treatment step is not essential). After removing the supernatant in the same manner as in the former step, 200  $\mu$ L/well of 50% methanol was added and it was left for 15 min at room temperature. Then all the supernatant was removed, 200  $\mu$ L/well of 50% methanol was added again, and the plate was left at room temperature for 20 min. After removing all of the supernatant, 200  $\mu$ L/well of 0.05 mol/L sucrose was added to avoid cell aggregation in the following cell-drying step. Then the supernatant was removed, leaving approximately 50  $\mu$ L of the solution, and then the solution was removed completely with an aspirator equipped with an 8-channel adaptor. The plate was completely dried by blowing with a hair-drier at room temperature (Additional file 1: Figure S1). After an additional fixation with 150  $\mu$ L/well of 99.5% methanol for 5 min, all of the methanol was removed and the plate was placed upside down on a paper towel. The plate was dried by blowing with a hair-drier and was stored in a plastic bag at -30 °C.

To compare the number of MNed cells counted by automatic imaging analysis with that counted manually with a microscope, conventional glass slide specimens were prepared by cytospin centrifugation of MMC-treated TK6 cells. Aliquots of the cell suspensions for the glass slide specimens were used as for the imaging analysis in a 96-well plate specimen by the method described above.

#### Immunostaining of $\gamma$ H2AX

The fluorescence immunostaining was conducted automatically using a microplate washer dispenser (EL406, BioTek Instruments, Winooski, VT, USA) under a programmed protocol. The plate was blocked

with 1% bovine serum albumin in PBS (BSA/PBS) for 1 h at room temperature. After removal of the solution, 50  $\mu\text{L}$ /well of anti- $\gamma\text{H2AX}$  (anti- $\gamma\text{H2AX}$ , phospho Ser139, mouse IgG [9F3], Abcam, Cambridge, UK) that had been diluted at 1:2000 with 1% BSA/PBS was added to each well and left for 2 h at room temperature. The plate was washed with PBS 3 times, and 50  $\mu\text{L}$ /well of AlexaFluor488-labeled anti-mouse IgG goat antibody (Invitrogen) that had been diluted at 1:2000 with 1% BSA/PBS was added to each well, and then the plate was placed at room temperature for 2 h. After washing with PBS 3 times, the plate was fixed with 150  $\mu\text{L}$ /well of 99.5% methanol for 5 min at room temperature. The methanol was removed and the air-dried plate was stored at  $-30\text{ }^{\circ}\text{C}$  until the time for staining. The plate was stained with 100  $\mu\text{L}$ /well of PBS containing 1.4  $\mu\text{g}/\text{mL}$  Hoechst33258 (Sigma) and 0.1 or 0.02  $\mu\text{g}/\text{mL}$  CellMask Red (Invitrogen). The plate was stored at  $4\text{ }^{\circ}\text{C}$  until imaging.

#### Imaging analysis

In Cell Analyzer 6000 (GE Healthcare) was used to capture images and KiNEDx (Peak Robotics, Colorado

Springs, CO, USA) was used to dispense plates automatically. Excitation filters used were as follows: a UV filter for primary nuclei or MNi stained with Hoechst33258, a blue filter for  $\gamma\text{H2AX}$  foci visualized by an Alexa Fluor488-labeled antibody, and a green filter for cytoplasm stained with CellMask Red. A 20-magnification objective lens was used to detect MNi and  $\gamma\text{H2AX}$  foci, and a 4- or 20-magnification lens was also used for counting cell numbers. Up to around 1000 cells per well, a total of 3000 cells in 3 wells, were analyzed at each dose to calculate the incidence of MNed cells and to count the  $\gamma\text{H2AX}$  foci per cell. Cells with pan-nucleic  $\gamma\text{H2AX}$  staining, which is mainly caused by apoptosis, were excluded from the calculation. M-phase cells were morphologically distinguished from cells in other cell-cycle phases and excluded from  $\gamma\text{H2AX}$  analysis, because M-phase cells are known to express  $\gamma\text{H2AX}$  independently of DNA damage response. Cell counts per image field were measured to calculate the percentage of RCC, which was an indicator of the cytotoxicity of each chemical. By using the doubling time of the TK6 cells, which was 14 h in the facility, the nominal cell count at the

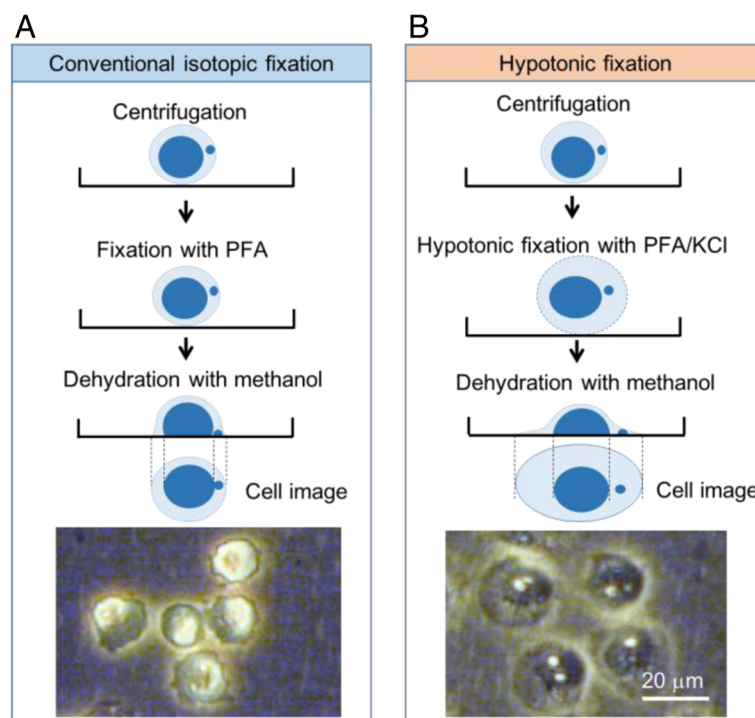


**Fig. 1** Schema of cell fixation methods and phase-contrast images of TK6 cells on the bottom of a well in the 96-well plate. **a** Fixation by a conventional method using an isotopic condition. Cells in the well were centrifuged and fixed with isotopic paraformaldehyde (PFA). Then the cells were dehydrated with methanol and became attached to the bottom of the well. The method caused cells to shrink through dehydration, and MNi were placed very close to the primary nuclei, which could make it difficult to detect MNi automatically by an imaging algorithm. **b** Fixation by the hypotonic process established in this study. Cells were fixed with hypotonic 1% PFA in 0.075 mol/L KCl (PFA/KCl). The swollen cells spread across the bottom of the well during dehydration. The separation of MNi from the primary nuclei made it easy to detect MNi automatically.

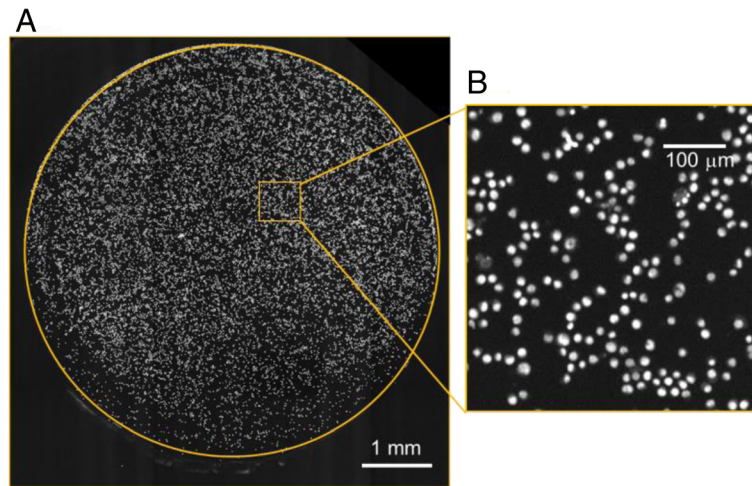


**Fig. 2** Representative images of TK6 cells attached on the bottom of a 96-well plate. **a** An image of a whole well in the plate and **b** a magnified image of nuclei stained with Hoechst33258. Cells were evenly dispersed and attached on the bottom. The cell binding was tight enough to endure the repeated machine-washings used when immunostaining  $\gamma$ H2AX

start of culturing and the percentage of RICC was calculated as well.

Cells treated with the chemicals for 24 h were classified to each cell-cycle stage by their fluorescent intensity and the shape of the nucleus. Cell-cycle arrest

was evaluated at the concentration where no severe cytotoxicity was observed. The cell cycle of cells treated for 3 h or 4 h was not analyzed because the treatment period would have been too short to affect the cell cycle [14, 15].

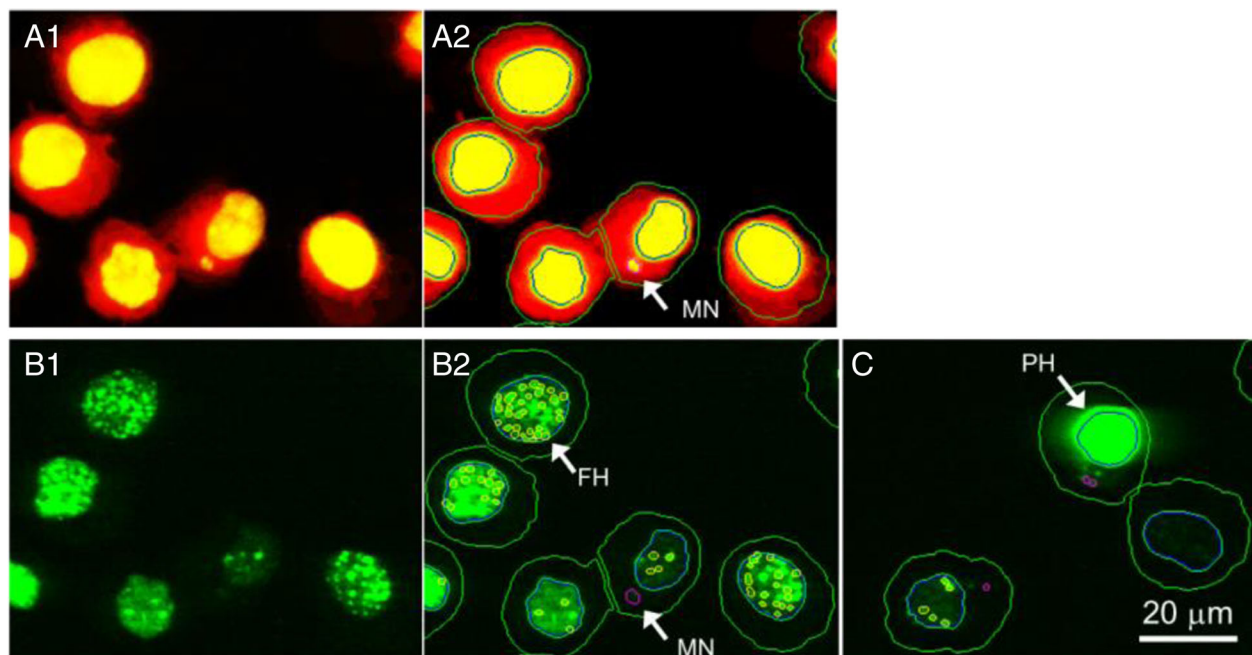


**Fig. 3** Representative images captured with an imaging cytometer of TK6 cells. Images other than C were obtained at the same time, from the same well. (A1) TK6 cells stained with Hoechst33258 for nuclei and CellMask Red for cytoplasm. The original monochrome images were given pseudo colors, yellow for nuclei and red for cytoplasm. (A2) The arrow shows a MN detected by automatic imaging analysis. (B1)  $\gamma$ H2AX foci stained immunocytochemically with AlexaFluor 488-labeled antibody. (B2) Foci of  $\gamma$ H2AX (FH) were detected by imaging-analysis. The  $\gamma$ H2AX foci and MNi were simultaneously detected by the common protocol of imaging analysis. (C) Pan-nuclear staining of  $\gamma$ H2AX (PH), which would be induced in apoptotic cells, was excluded from the analyses

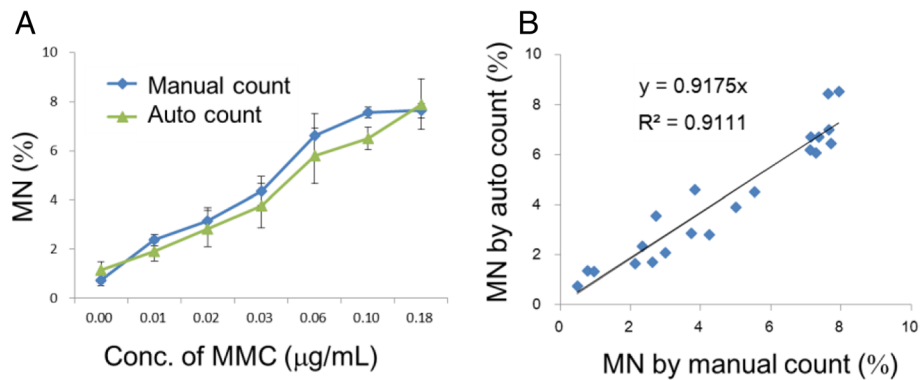


**Fig. 4** Correlation between scoring MN manually and scoring MN automatically with the imaging-analysis algorithm. MNed TK6 cells treated with MMC were scored manually in specimens on glass slides or automatically using 96-well plates. **a** Percentage of MNed cells increased in a dose-related manner in parallel when scored either manually or automatically. **b** All individual data on MNed cell % were plotted to confirm the correlation between these methods

The chemical was judged as positive in the MN test if the incidence of MNed cells (average of 3 wells) increased to twice or more than that of the concurrent control and if the increase was dose-dependent. When the  $\gamma$ H2AX focus count per cell increased to twice or more than that of the concurrent control and the increase was dose-dependent, the chemical was judged as positive for  $\gamma$ H2AX induction.

**Results**

**Preparation of plate specimens and imaging analysis**

Fixation of TK6 cells on the bottom of 96-well plates was successfully achieved by the protocol established in this study (Fig. 1). When images of cells fixed with the generally-used isotopic PFA were compared with those fixed hypotonically with PFA/KCl, cell shrinkage was obviously improved. As shown in Fig. 2, the cells were

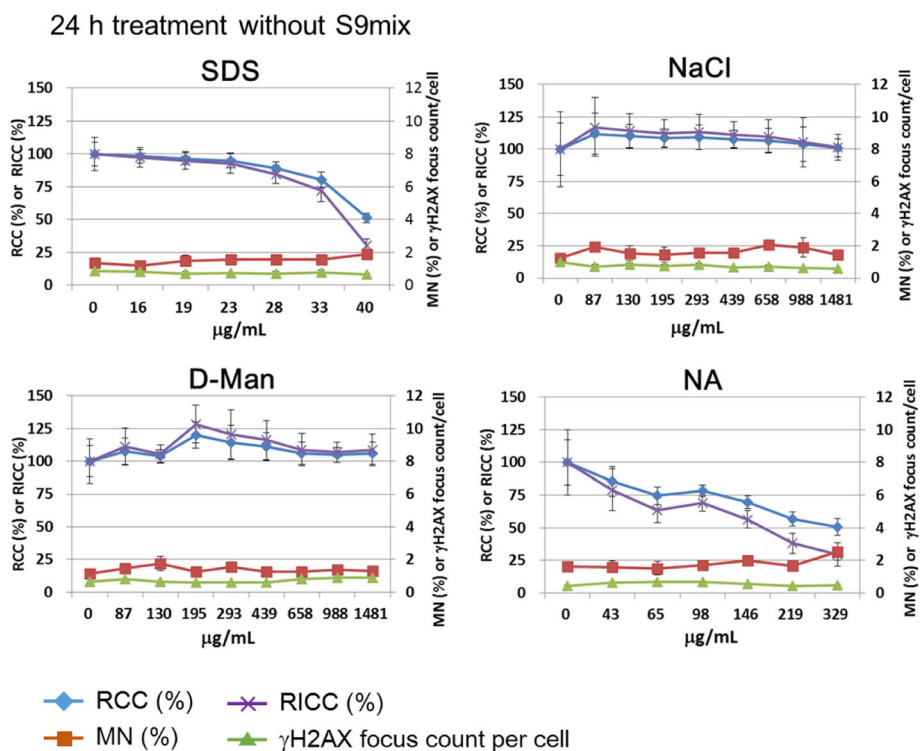
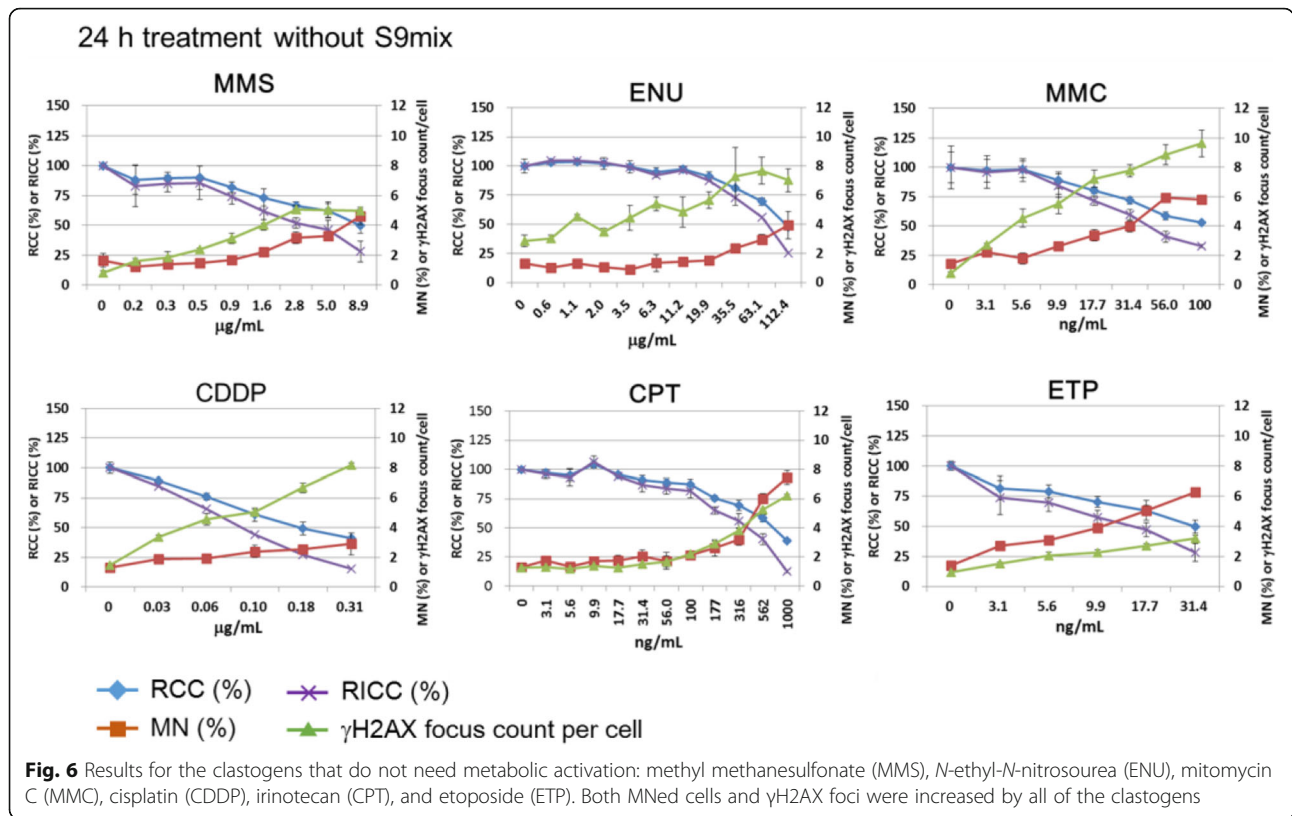


**Fig. 5** The results of non-genotoxins, sodium dodecyl sulfate (SDS), sodium chloride (NaCl), D-mannitol (D-Man), and nalidixic acid (NA). The blue and purple lines represent relative cell count (RCC) and relative increase of cell count (RICC), respectively. The red and green lines show percentage of MNed cells and  $\gamma$ H2AX focus counts per cell, respectively. Non-genotoxins did not induce either MNi or  $\gamma$ H2AX foci



dispersed evenly on the bottom of each well without aggregation or stacking. Furthermore, over 80% of seeded cells became attached to the bottom of wells (data not shown).

Typical examples from the imaging analyses are shown in Fig. 3 and Additional file 1: Figures S2-S5. When conditions were without S9 mix, both MNi and γH2AX foci were analyzed simultaneously using the common image sources (when S9 mix was used, the images taken to detect MNi and γH2AX foci were different because the treatment regimen was different). MNi could be detected as vesicles in the area between the primary nucleus and the outside boundaries of cytoplasm. Foci of γH2AX could be detected as vesicles in the area of the primary nucleus.

**Comparison with manual MN counting**

A high correlation ( $R^2 = 0.91$ ) was observed between the frequency of MMC-induced MNed cells measured by the automatic imaging analysis on a 96-well plate and that found by skilled observers manually counting cells on the glass slides by microscope (Fig. 4).

**Measurement of MNed cell frequency and γH2AX focus count**

The results of MNed cell frequency and γH2AX focus count per cell are shown in Figs. 5, 6, 7 and 8. The summary of the

results is shown in Table 2. Details of the results of each group, non-genotoxins, clastogens, and aneugens, are described below.

**Non-genotoxins**

The cells were treated with each non-genotoxin for 24 h without S9 to detect γH2AX foci and MNi. None of the non-genotoxins tested increased the frequency of MNed cells or γH2AX foci (Fig. 5). Treatment with SDS or NA reduced RCC or RICC to 50% or less. Treatment with NaCl or D-Man did not show cytotoxicity even at concentrations higher than 0.5 mg/mL which is the highest dose stipulated for in vitro cytogenesis tests in the ICH S2(R1) guideline. Therefore, all the non-genotoxins tested in this study were judged correctly as negative.

**Clastogens**

The cells were treated with each clastogen (MMS, ENU, MMC, CDDP, CPT, and ETP) for 24 h without S9 to detect γH2AX foci and MNi. The cells were also treated with BaP, CP, or PhIP for 4 h with S9 to detect γH2AX foci or for 3 h with S9 followed by a 21 h recovery to detect MNi. All the clastogens tested increased the frequency of both MNed cells and γH2AX foci at the concentrations that reduced RCC up to around 50% (Figs. 6 and 7). Therefore, all the

3 h treatment with S9mix and 21 h recovery

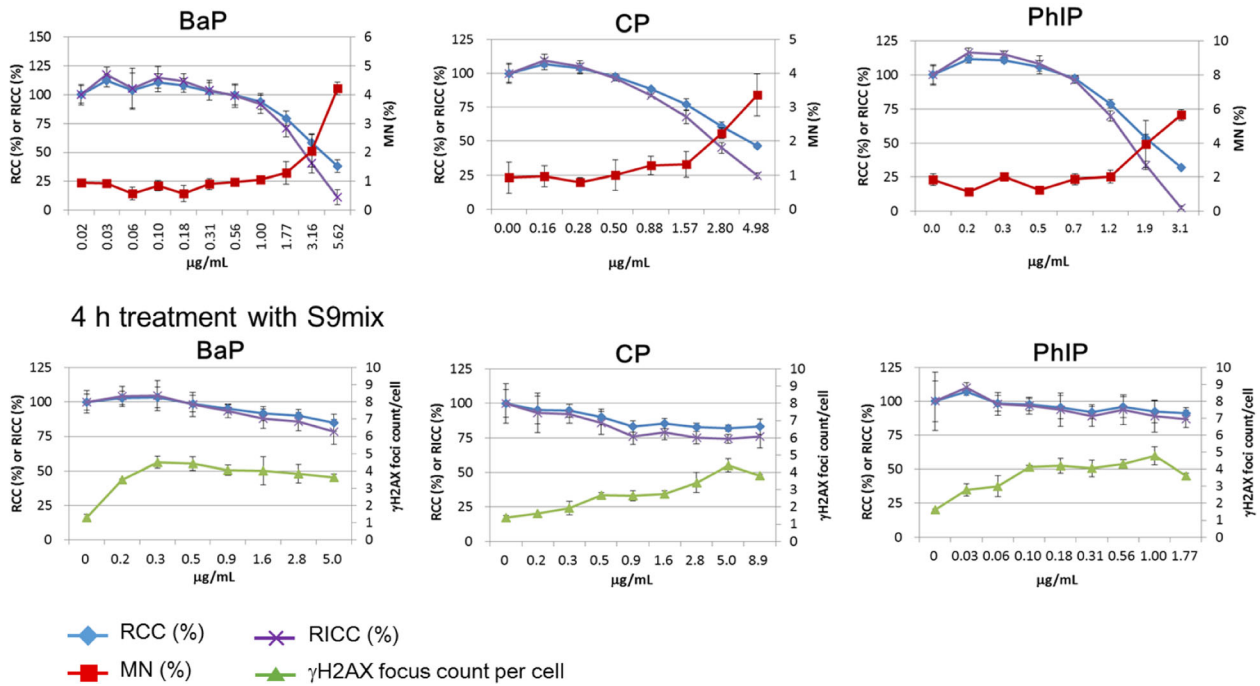


**Fig. 7** Results for the clastogens that need metabolic activation: benzo[*a*]pyrene (BaP), cyclophosphamide (CP), and 2-amino-1-methyl-6-phenylimidazo[4,5-*b*]pyridine hydrochloride (PhIP). MNed cells were measured after treatment with each chemical and with S9 mix for 3 h followed by recovery culture for 21 h.  $\gamma$ H2AX foci were measured after 4 h treatment with each chemical with S9 mix. Both MNed cells and  $\gamma$ H2AX foci were increased by all of the clastogens

24 h treatment without S9mix

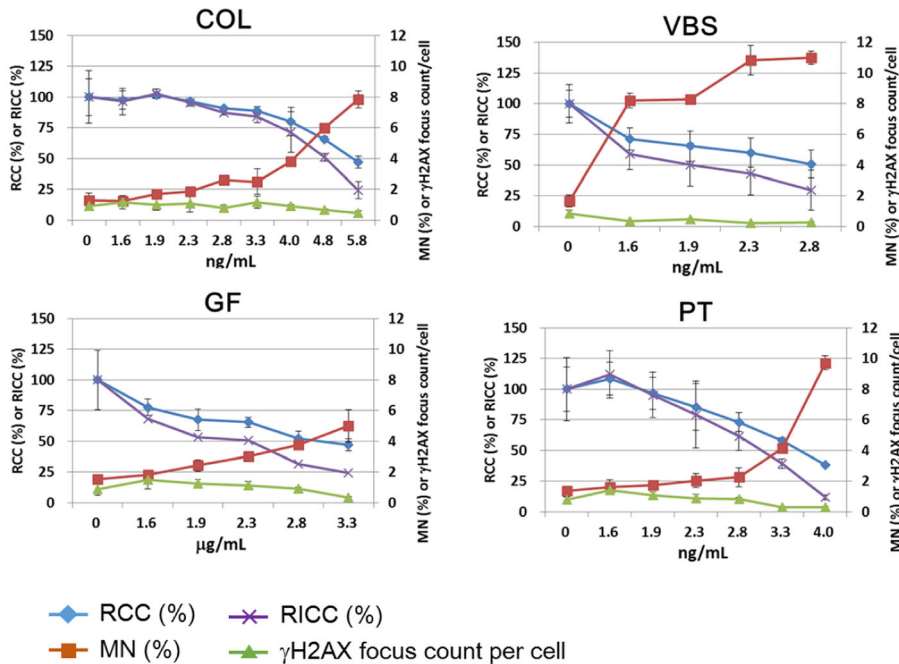


**Fig. 8** Results for the aneugens colchicine (COL), vinblastine sulfate (VBS), griseofulvin (GF), and paclitaxel (PT). These aneugens induced MNed cells while  $\gamma$ H2AX foci were not induced

**Table 2** Summary of the induction of MNi and  $\gamma$ H2AX foci

| Class          | Chemicals | Results      |                               |
|----------------|-----------|--------------|-------------------------------|
|                |           | MN induction | $\gamma$ H2AX focus induction |
| Non-genotoxins | SDS       | Neg.         | Neg.                          |
|                | NaCl      | Neg.         | Neg.                          |
|                | D-Man     | Neg.         | Neg.                          |
|                | NA        | Neg.         | Neg.                          |
| Clastogens     | MMS       | Pos.         | Pos.                          |
|                | ENU       | Pos.         | Pos.                          |
|                | MMC       | Pos.         | Pos.                          |
|                | CDDP      | Pos.         | Pos.                          |
|                | CPT       | Pos.         | Pos.                          |
|                | ETP       | Pos.         | Pos.                          |
|                | BaP       | Pos.         | Pos.                          |
|                | CP        | Pos.         | Pos.                          |
|                | PhIP      | Pos.         | Pos.                          |
| Aneugens       | COL       | Pos.         | Neg.                          |
|                | VBS       | Pos.         | Neg.                          |
|                | GF        | Pos.         | Neg.                          |
|                | PT        | Pos.         | Neg.                          |

clastogens tested in this study were judged correctly as positive. The induction of  $\gamma$ H2AX foci suggested that all the clastogens tested, or their metabolites activated by S9 mix, directly damaged DNA.

### Aneugens

The cells were treated with each aneugen for 24 h without S9 to detect  $\gamma$ H2AX foci and MNi. All the aneugens increased MNed cell frequency in the concentration range at which RCC or RICC was reduced to around 50% or less (Fig. 8). Therefore, all the aneugens tested were correctly judged as positive in the MN test. However, none of the aneugens increased  $\gamma$ H2AX focus count, even at the concentrations at which RCC or RICC was reduced to 50% or less. These findings suggested that MN induction by the aneugens was not accompanied by direct DNA damage.

### Cell cycle

The result of cell-cycle analysis is presented in Fig. 9. Treatment with D-Man did not show cell-cycle arrest, but cells treated with SDS, NaCl, and NA showed G1 phase arrest, VBS, GF, and PT showed M/G1 arrest, ENU showed G2 arrest, and MMS, MMC, CDDP, CPT, ETP, and COL showed G2/M arrest. COL also increased G1 cells at the mid concentrations.

### Discussion

In the present study, we established a high-throughput genotoxicity test system in which TK6 cells were spread

and fixed on the bottom of 96-well plates (Figs. 1 and 2). The system was able to simultaneously analyze the incidence of MNed cells and  $\gamma$ H2AX foci (Fig. 3). The incidence of MNed cells detected automatically by the system correlated highly with that of conventional manual scoring by microscope (Fig. 4), and the assay system judged all the non-genotoxins and genotoxins used in the study correctly (Table 2). Therefore, the assay system was suggested to have enough sensitivity and specificity to practically detect the genotoxicity of chemicals. Furthermore, when  $\gamma$ H2AX focus evaluation and MNed cell detection were combined, aneugens were clearly discriminated from clastogens. As shown in Fig. 10, when the chemicals used in the study were plotted by the fold-increase of MNed cells and that of  $\gamma$ H2AX focus count per cell, the chemicals in each class—non-genotoxin, clastogen, and aneugen—were clearly plotted in their characteristic area. Moreover, cell-cycle analysis was feasible in the assay system (Fig. 9). Taken together, the results suggest that the assay system established in this study is a powerful tool for genotoxicity screening in pharmaceutical development or to identify risk in a large number of industrial or environmental chemicals.

So far, several high-throughput MN detection systems have been reported. Verma et al. reported a system for scoring MN in TK6 cells that combined the flow-cytometric MicroFlow method and the Metafer system, which is based on glass slides [16]. Ogata et al. reported an imaging-based MN scoring test system in CHL/IU cells [10]. Westerink et al. reported an imaging-based MN screening system using CHO-k1 and HepG2 cells [11]. Thougard et al. presented a validation result of the MicroFlow system for MN detection in TK6 cells [17]. Bryce et al. established a flow-cytometric multiplex test system that detected p53, phospho-H3, and 8 N cells to clarify whether the genotoxic mode of action in TK6 cells was aneugenic or clastogenic [18]. The characteristics of these test systems are summarized in Table 3.

Conventional MN tests are based on manual observation through a microscope [19, 20] by skilled observers, who determine whether vesicles in cytoplasm are bona fide MNi. These observers use the information from MN images, such as morphology, size, and roundness, to discriminate bona fide MNi from MN-like vesicles, such as cell debris, fragments of apoptotic nuclei, or auto-fluorescence of chemical precipitates. An advantage of imaging-based automatic MN detection systems is that the standards of MN qualification it applies are in common with the manual method [10, 11, 16]; therefore, the validity of an imaging algorithm used to detect MNi can be easily confirmed by comparing the number of MNi it detects with that detected by skilled observers. Moreover, all images captured by imaging-based methods can generally be stored as digital data, so that re-analysis of the data by a modified algorithm is feasible. On the downside, however, the imaging-based

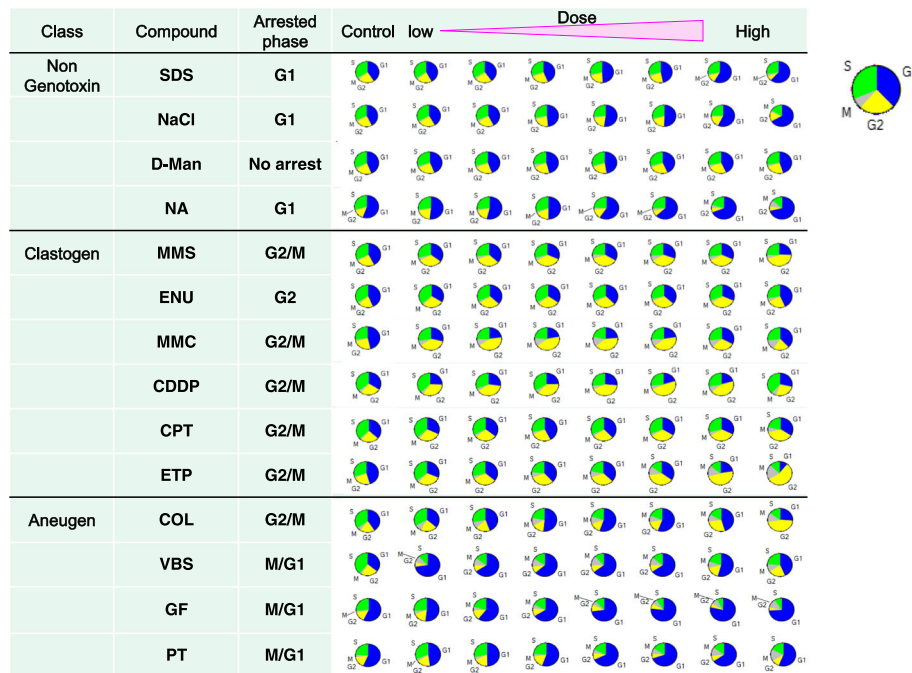


**Fig. 9** The results of cell-cycle analyses of the chemicals used in the study. The ratio of cells in each cell-cycle phase is shown as a pie-chart that describes the result derived from up to around 1000 cells in a representative well of the 96-well plate. The wells at low to high dose levels are aligned from left to right (the well at the left end represents the concurrent control), the phase at which cell cycle was arrested by treatment with each chemical is also indicated

high-throughput assays reported so far can only use adherent cell lines. Though an advantage of the TK6 cell line is the low rate of false positives probably due to intact p53 [13], its use in an imaging-based high-throughput assay is limited because the non-adherent cells are difficult to fix on

the bottom of multi-well plates. In fact, the TK6 cell line can be used with the imaging-based Metafer assay [16], but since the assay uses glass-slide specimens, the throughput is only mid-range. Flowcytometry (FCM)-based assays have the advantage of allowing multi-endpoint analysis [18], but

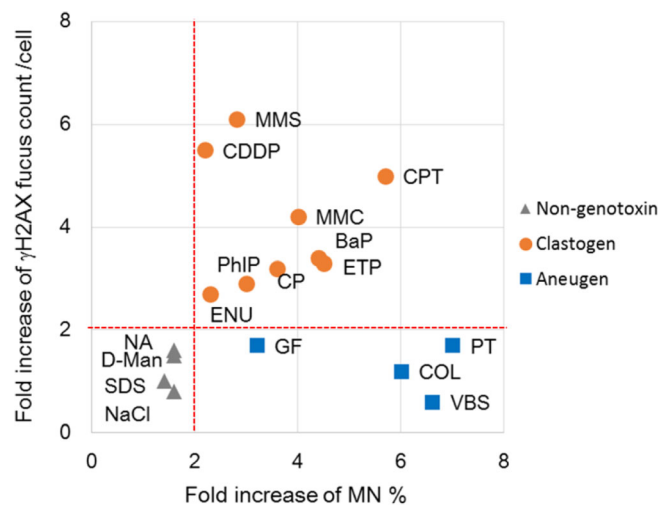


**Fig. 10** Scatter plots of the chemicals used in the study. The horizontal axis represents fold increase of MN % from each concurrent control level. The vertical axis shows fold increase of  $\gamma$ H2AX focus count per cell from each control level. The broken red lines indicate the thresholds for judging positive or negative for MN or  $\gamma$ H2AX foci induction, which were 2-fold of control levels. The non-genotoxins are plotted in the lower-left area, which means neither MN nor  $\gamma$ H2AX foci was induced. The clastogens are plotted in the upper-right area, while the aneugens are plotted in the lower-right area. This reflects that clastogens induced both MN and  $\gamma$ H2AX, but aneugens induced MN without any induction of  $\gamma$ H2AX

**Table 3** Characteristics of automatic MN detection methods

| Methods for MN detection   | Advantage  | Limitation  | Reference    |
|--|--|---|--------------|
| Imaging analysis with slide glass specimens  | Easy to confirm the validity of a MN-detection algorithm by means of checking the MN images manually by skilled observers.   | Limited to middle-throughput. Difficult to apply multi-endpoint assays.<br><br>Difficult to apply robotics for plate preparation. | 16           |
| Imaging analysis with micro-plates in adherent cells                                 | Easy to confirm the validity of an algorithm by means of checking the MN images manually by skilled observers.<br><br>Easy to apply robotics for plate preparation.            | Difficult to apply to non-adherent cells such as TK6 or primary lymphocytes.  | 10, 11       |
| Flowcytometric analysis  | Easy to apply to non-adherent cells such as TK6 or primary lymphocytes. Applicable to multi-endpoint assay (e.g. $\gamma$ H2AX, H3, p53).                                      | Difficult to confirm whether the MN detected were bona fide.<br><br>Difficult to apply robotics for the sample preparation.       | 18           |
| Imaging analysis with micro-plate in non-adherent cells (the method in this article) | Easy to confirm the validity of an algorithm by means of checking the MN images manually by skilled observers.<br><br>Applicable to multi-endpoint assay (e.g. $\gamma$ H2AX). | Difficult to apply robotics for plate preparation.  | This article |

it is difficult to confirm whether the MNi detected by FCM are bona fide ones or to re-analyze the data once obtained. In summary, the advantages of using the method established in this study are that it uses the TK6 cell line, which has a low rate of false positives, and it is easy to validate the imaging algorithm.

The use of  $\gamma$ H2AX as an endpoint of genotoxicity evaluation has good compatibility with high-throughput platforms because it is induced by a broad range of genotoxic events, such as DSB, SSB, or DNA replication stall, and the foci can easily be specifically detected by fluorescent immunostaining. High-throughput genotoxicity assay systems that use  $\gamma$ H2AX as a single endpoint have been reported [21–24]. Furthermore,  $\gamma$ H2AX has been used in combination with cellular function as another endpoint. Ando et al. showed that combining  $\gamma$ H2AX evaluation with cell-cycle analysis was effective to reveal the genotoxic mode of action [25]. Khoury et al. reported that the combination of  $\gamma$ H2AX with phosphorylation of histone H3 at Ser10 was effective to distinguish aneugens from clastogens in 3 cell lines, including HepG2 [26]. In this study, we combined  $\gamma$ H2AX with MN detection in TK6 cells and this is the first report of using this combination in an imaging-based high-throughput assay system. The assay system we report here could provide multi-endpoint data, such as MNi,  $\gamma$ H2AX, and cell-cycle analysis, from a single 96-well plate specimen. Adding further endpoints is feasible, if appropriate antibodies to detect those endpoints are selected such as phosphorylated histone H3. On the other hand, our method is limited at the present time by the availability of robotics that can prepare the plate specimens, because many experimental steps, including repeated centrifugations and washings,

are needed to attach the non-adherent cells to the bottom of the 96-well plate.

The results of MN,  $\gamma$ H2AX, and cell-cycle analysis in this report were compared with those in previous reports. MN induction was reported as positive in TK6 cells treated with MMC, COL, VBS, BaP, CP [27], ETP [28], MMS [29], CDDP, and PT [30], but was negative in TK6 cells treated with NA and NaCl [27]. The data contained in our report are consistent with these previous reports in TK6 cells. Furthermore, MN induction by CPT was reported in human peripheral lymphocytes [31] and V79 [32], and by GF in CHL and L5178Y [33]. PhIP was reported to induce MNed V79 cells [34]. D-Man was negative in a MN test using human peripheral lymphocytes [35]. The results in our report are also consistent with these previous reports. With regard to SDS, we could not find any reports of the in vitro MN induction of this compound, so we presume that our negative result for SDS is plausible.

Induction of  $\gamma$ H2AX in TK6 cells was previously reported by Bryce et al. [35]. The clastogens they used included MMS, MMC, CDDP, ETP, BaP, and CP, which all induced  $\gamma$ H2AX, but the aneugens PT, VBS, COL, and GF and the non-genotoxins SDS, NaCl, and D-Man did not induce  $\gamma$ H2AX.  $\gamma$ H2AX was induced in human amnion FL cells treated with ENU [36] and in NCI-60 cancer cells treated with CPT [37]. PhIP increased  $\gamma$ H2AX foci in V79 cells expressing CYP1A2 and SULT1A1 [38]. No reports on the induction of  $\gamma$ H2AX by NA were found. However, NA was reported negative in a GADD45 $\beta$  assay in HepG2 cells [39], an in vitro comet assay, and an in vitro MN test in WTK-1 cells [40]. Therefore, our data is consistent with these previous reports.

Cell cycle was analyzed in TK6 cells in a couple of previous reports. MMS and MMC induced arrest in the G2 or M phase (G2/M) [15] and VBS induced arrest in the M phase [41], and our results are consistent with these previous reports. In our results, ETP induced G2/M phase arrest in TK6 cells. In other reports, TK6 cells were arrested in the S phase immediately after treatment with ETP while in a recovery period, and G2 phase cells increased [41]. Moreover, ETP was reported to induce G2/M phase arrest in 3T3-L1 mouse cells [42]. Therefore, our present finding of G2/M phase arrest in TK6 is thought to be plausible. In A549 cells, CDDP [43] and COL [44] were reported to induce G2/M phase arrest. Although COL mainly induced G2/M arrest, an increase in G1 cells at the mid concentrations was also observed. Nocodazole and vincristine which are microtubule-depolymerizing agents similar to COL were reported to induce mitotic arrest at low concentrations, while G1 and G2 arrest were also induced at higher concentrations in some cell lines [45]. The same mechanisms might underlie the increase in G1 cells observed at the mid concentrations of COL. PT was reported to induce G1 phase arrest in primary fibroblasts of rat or human [46]. NaCl increased the ratio of G1 phase at high concentrations [47]. Therefore our present results are consistent with these previous reports. Although CPT induced G2/M phase arrest in our study, S phase arrest in MCF-7 cells [48] and S phase and G2/M arrest in Caco-2 cells and CW cells have been reported [49]. In our study, GF induced M/G1 arrest, whereas G2/M phase arrest was reported in HL-60 cells [50]. Though, the reason for the discrepancy between our results and these previous reports is unclear, the difference may be related to the cell line used. Though ENU induced G2 arrest in our study, the reagent was reported to induce S phase arrest in neural progenitor cells derived from rat or mouse [51]. In the previous report, the peak of increase in S phase cells was 6 h after the initiation of treatment; however, the cells in our study were treated for 24 h and no S phase arrest was observed. Therefore the discrepancy in cell-cycle arrest may come from the difference in experimental conditions. In our present study, NA and SDS induced G1 arrest, and D-Man did not induce any cell-cycle arrest. However as far as we know, there is no report about cell-cycle arrest induced by these reagents.

## Conclusion

A HC imaging assay to detect  $\gamma$ H2AX foci and MNi was established in the TK6 cell line, which is recommended for use in the OECD guideline and is reported to rarely exhibit false-positive results. The assay provided information on the aneugenic/clastogenic mode of action and on cell-cycle arrest. Therefore, the assay is expected to

be a useful tool for high-throughput screenings of genotoxicity and its MOA.

## Additional file

**Additional file 1: Figure S1.** A handmade adaptor was used to dry plates with a hair-drier. Pictures A1–A6 explain the method to assemble the adaptor. (A2) Bottoms of a 96-well PCR tube plate were removed with nipper pliers to make small ducts. (A3) A hole the size of the mouth of the hair-drier was cut in an empty box of 96 micro-pipette tips. (A4) The PCR tube plate and the empty box were connected with adhesive tape. (A5, A6) The adaptor was attached to the hair-drier. (B) Each duct of the PCR tube was aligned with each well of the 96-well plates to directly blow the bottom of the well. **Figure S2.** A typical image captured by In Cell analyzer 6000 (GE Healthcare). TK6 cells attached on the bottom of a 96-well plate. The image shows nuclei stained with Hoechst 33258. The Figs. S2 to S5 represent the images obtained from the same cells at the same time. **Figure S3.** Cytoplasm stained with CellMask Red. The image was used to identify the boundaries of the cells. **Figure S4.** Fluorescent immunostaining with anti- $\gamma$ H2AX antibody. **Figure S5.** Imaging analysis by the software 'Developer' (GE Healthcare). Light blue and green lines show the boundaries of nuclei and cytoplasm, respectively. Yellow circles represent foci of  $\gamma$ H2AX. A MN is shown as a red circle, marked with an arrow labelled MN at center top. M phase cells (M) and apoptotic cells (AP) were excluded from  $\gamma$ H2AX foci counting. (DOC 20237 kb)

## Abbreviations

BaP: benzo[*a*]pyrene; BSA: Bovine serum albumin; CDDP: Cisplatin; COL: Colchicine; CP: Cyclophosphamide; CPT: Irinotecan; D-Man: D-mannitol; DMSO: Dimethyl sulfoxide; DSB: DNA double-strand break; ENU: *N*-ethyl-*N*-nitrosourea; ETP: Etoposide; FBS: Fetal bovine serum; FCM: Flowcytometry; GF: Griseofulvin; HC: High-content; KCl: Potassium chloride; MMC: Mitomycin C; MMS: Methyl methanesulfonate; MN: Micronucleus; MNed: Micronucleated; MNi: Micronuclei; MoA: Mode of action; NA: Nalidixic acid; NaCl: Sodium chloride; PBS: Phosphate buffered saline; PFA: Paraformaldehyde; PHIP: 2-amino-1-methyl-6-phenylimidazo[4,5-*b*]pyridine hydrochloride; PT: Paclitaxel; RCC: Relative cell counts; RICC: Relative increase of cell counts; SDS: Sodium dodecyl sulfate; SSB: DNA single-strand break; VBS: Vinblastine sulfate salt

## Acknowledgements

Authors thank Dr. Mitsuyasu Tabo and Dr. Shuichi Chiba of Chugai Pharmaceutical Co., Ltd. for critically reading the manuscript. The authors would like to thank Dr. Andreas Zeller, Dr. Stephan Kirchner, and Dr. Melanie Guérard of F. Hoffmann-La Roche Ltd. for their helpful advice. Authors also thank Ms. Sally Matsuura of Chugai Pharmaceutical Co., Ltd. for her technical editing. The technical help of many contributors to this work is acknowledged.

## Funding

All the present study was funded by Chugai Pharmaceutical Co., Ltd.

## Availability of data and materials

The datasets generated and analyzed during the current study are available from the corresponding author on reasonable request.

## Conflict of interests

Authors are employed at the company funding the research.

## Authors' contributions

AT, KM, SM, MY, AH, CK, KT were involved in data collection. AT and KM contributed to analyzing the data and drafting the manuscript. AT and MM contributed to the data interpretation. All authors read and approved the final manuscript.

## Ethics approval and consent to participate

Not applicable.

## Consent for publication

Not applicable.

**Competing interests**

The authors declare that they have no competing interests.

**Publisher's Note**

Springer Nature remains neutral with regard to jurisdictional claims in published maps and institutional affiliations.

Received: 9 November 2018 Accepted: 7 January 2019

Published online: 05 February 2019

**References**

- OECD guideline for the testing of chemicals, *In vitro* mammalian cell micronucleus test, OECD/OCDE TG 487, 29 July 2016.
- Mishima M. Chromosomal aberrations, clastogens vs aneugens. *Front Biosci (Schol Ed)*. 2017;9:1–16.
- ICH steering committee, ICH harmonised tripartite guideline, Guidance on genotoxicity testing and data interpretation for pharmaceuticals intended for human use S2 (R1). 2011.
- Motoyama S, Takeiri A, Tanaka K, Harada A, Matsuzaki K, Taketo J, Matsuo S, Fujii E, Mishima M. Advantages of evaluating  $\gamma$ H2AX induction in non-clinical drug development. *Genes Environ*. 2018;40:10.
- Mishima M, Tanaka K, Takeiri A, Harada A, Kubo C, Sone S, Nishimura Y, Tachibana Y, Okazaki M. Two structurally distinct inhibitors of glycogen synthase kinase 3 induced centromere positive micronuclei in human lymphoblastoid TK6 cells. *Mutat Res*. 2008;643:29–35.
- Bonner WM, Redon CE, Dickey JS, Nakamura AJ, Sedelnikova OA, Solier S, Pommier Y.  $\gamma$ H2AX and cancer. *Nat Rev Cancer*. 2008;8:957–67.
- Dickey JS, Redon CE, Nakamura AJ, Baird BJ, Sedelnikova OA, Bonner WM. H2AX: functional roles and potential applications. *Chromosoma*. 2009;118:683–92.
- Solier S, Pommier Y. The nuclear  $\gamma$ -H2AX apoptotic ring: implications for cancers and autoimmune diseases. *Cell Mol Life Sci*. 2014;71:2289–97.
- Cleaver JE.  $\gamma$ H2AX: biomarker of damage or functional participant in DNA repair "all that glitters is not gold!". *Photochem Photobiol*. 2011;87:1230–9.
- Ogata AS, Kakinuma C, Hioki T, Kasahara T. Evaluation of high-throughput screening for *in vitro* micronucleus test using fluorescence-based cell imaging. *Mutagenesis*. 2011;26:709–19.
- Westerink WM, Schirris TJ, Horbach GJ, Schoonen WG. Development and validation of a high-content screening in vitro micronucleus assay in CHO-k1 and HepG2 cells. *Mutat Res*. 2011;724:7–21.
- Fowler P, Smith K, Young J, Jeffrey L, Kirkland D, Pfuhrer S, Carmichael P. Reduction of misleading ("false") positive results in mammalian cell genotoxicity assays. I. Choice of cell type. *Mutat Res*. 2012;742:11–25.
- Fowler P, Smith R, Smith K, Young J, Jeffrey L, Carmichael P, Kirkland D, Pfuhrer S. Reduction of misleading ("false") positive results in mammalian cell genotoxicity assays. III: sensitivity of human cell types to known genotoxic agents. *Mutat Res*. 2014;767:28–36.
- Bassi L, Carloni M, Fonti E, Palma de la Peña N, Meschini R, Palitti F. Pifithrin- $\alpha$ , an inhibitor of p53, enhances the genetic instability induced by etoposide (VP16) in human lymphoblastoid cells treated in vitro. *Mutat Res*. 2002;499:163–76.
- Islaih M, Halstead BW, Kadura IA, Li B, Reid-Hubbard JL, Flick L, Altizer JL, Thom Deahl J, Monteith DK, Newton RK, Watson DE. Relationships between genomic, cell cycle, and mutagenic responses of TK6 cells exposed to DNA damaging chemicals. *Mutat Res*. 2005;578:100–16.
- Verma JR, Rees BJ, Wilde EC, Thornton CA, Jenkins GJS, Doak SH, Johnson GE. Evaluation of the automated MicroFlow<sup>®</sup> and Metafer<sup>™</sup> platforms for high-throughput micronucleus scoring and dose response analysis in human lymphoblastoid TK6 cells. *Arch Toxicol*. 2017;91:2689–98.
- Thougaard AV, Christiansen J, Mow T, Hornberg JJ. Validation of a high throughput flow cytometric in vitro micronucleus assay including assessment of metabolic activation in TK6 cells. *Environ Mol Mutagen*. 2014;55:704–18.
- Bryce SM, Bernacki DT, Bemis JC, Spellman RA, Engel ME, Schuler M, Lorge E, Heikkinen PT, Hemmann U, Thybaud V, Wilde S, Queisser N, Sutter A, Zeller A, Guérard M, Kirkland D, Dertinger SD. Interlaboratory evaluation of a multiplexed high information content in vitro genotoxicity assay. *Environ Mol Mutagen*. 2017;58:146–61.
- Hayashi M. The micronucleus test-most widely used *in vivo* genotoxicity test. *Genes Environ*. 2016;38:18.
- Yamamoto A, Hirouchi T, Kawamorita S, Nakashima K, Sugiyama A, Kato Y. Radioprotective activity of blackcurrant extract evaluated by in vitro micronucleus and gene mutation assays in TK6 human lymphoblastoid cells. *Genes Environ*. 2017;39:22.
- Smart DJ, Ahmedi KP, Harvey JS, Lynch AM. Genotoxicity screening via the  $\gamma$ H2AX by flow assay. *Mutat Res*. 2011;715:25–31.
- García-Canton C, Anadon A, Meredith C. Assessment of the *in vitro*  $\gamma$ H2AX assay by high content screening as a novel genotoxicity test. *Mutat Res*. 2013;757:158–66.
- Tsamou M, Jennen DG, Claessen SM, Magkoufopoulou C, Kleinjans JC, van Delft JH. Performance of in vitro  $\gamma$ H2AX assay in HepG2 cells to predict in vivo genotoxicity. *Mutagenesis*. 2012;27:645–52.
- Matsuzaki K, Harada A, Takeiri A, Tanaka K, Mishima M. Whole cell-ELISA to measure the  $\gamma$ H2AX response of six aneugens and eight DNA-damaging chemicals. *Mutat Res*. 2010;700:71–9.
- Ando M, Yoshikawa K, Iwase Y, Ishiura S. Usefulness of monitoring  $\gamma$ -H2AX and cell cycle arrest in HepG2 cells for estimating genotoxicity using a high-content analysis system. *J Biomol Screen*. 2014;19:1246–54.
- Khouri L, Zalko D, Audebert M. Complementarity of phosphorylated histones H2AX and H3 quantification in different cell lines for genotoxicity screening. *Arch Toxicol*. 2016;90:1983–95.
- Sobol Z, Homiski ML, Dickinson DA, Spellman RA, Li D, Scott A, Cheung JR, Coffing SL, Munzner JB, Sanok KE, Gunther WC, Dobo KL, Schuler M. Development and validation of an in vitro micronucleus assay platform in TK6 cells. *Mutat Res*. 2012;746:29–34.
- Elhajouji A. Mitomycin C, 5-fluorouracil, colchicine and etoposide tested in the in vitro mammalian cell micronucleus test (MNvit) in the human lymphoblastoid cell line TK6 at Novartis in support of OECD draft test guideline 487. *Mutat Res*. 2010;702:157–62.
- Yamamoto M, Wakata A, Aoki Y, Miyamae Y, Kodama S. Induction of a whole chromosome loss by colcemid in human cells elucidated by discrimination between FISH signal overlap and chromosome loss. *Mutat Res*. 2013;749:39–48.
- Le Fevre AC, Boitier E, Marchandeaude JP, Sarasin A, Thybaud V. Characterization of DNA reactive and non-DNA reactive anticancer drugs by gene expression profiling. *Mutat Res*. 2007;619:16–29.
- Kopjar N, Zeljezić D, Vrdoljak AL, Radić B, Ramić S, Milić M, Gamulin M, Pavlica V, Fucić A. Irinotecan toxicity to human blood cells *in vitro*: relationship between various biomarkers. *Basic Clin Pharmacol Toxicol*. 2007;100:403–13.
- Kasuba V, Rozgaj R, Gamulin M, Trošić I. Assessment of cyto/genotoxicity of irinotecan in v79 cells using the comet, micronucleus, and chromosome aberration assay. *Arh Hig Rada Toksikol*. 2010;61:1–9.
- Lorge E, Thybaud V, Aardema MJ, Oliver J, Wakata A, Lorenzon G, Marzin D. SFTG international collaborative study on in vitro micronucleus test I General conditions and overall conclusions of the study. *Mutat Res*. 2006;607:13–36.
- Perez C, Lopez de Cerain A, Bello J. Induction of micronuclei in V79 cells after combined treatments with heterocyclic aromatic amines. *Food Chem Toxicol*. 2002;40:1463–7.
- Bryce SM, Bernacki DT, Bemis JC, Dertinger SD. Genotoxic mode of action predictions from a multiplexed flow cytometric assay and a machine learning approach. *Environ Mol Mutagen*. 2016;57:171–89.
- Zhou C, Li Z, Diao H, Yu Y, Zhu W, Dai Y, Chen FF, Yang J. DNA damage evaluated by  $\gamma$ H2AX foci formation by a selective group of chemical/physical stressors. *Mutat Res*. 2006;604:8–18.
- Ji J, Zhang Y, Redon CE, Reinhold WC, Chen AP, Fogli LK, Holbeck SL, Parchment RE, Hollingshead M, Tomaszewski JE, Dudon Q, Pommier Y, Doroshov JH, Bonner WM. Phosphorylated fraction of H2AX as a measurement for DNA damage in cancer cells and potential applications of a novel assay. *PLoS One*. 2017;12:e0171582.
- Mimmeler M, Peter S, Kraus A, Strohs S, Nikolova T, Seiwert N, Hasselwander S, Neitzel C, Haub J, Monien BH, Nicken P, Steinberg P, Shay JW, Kaina B, Fahrner J. DNA damage response curtails detrimental replication stress and chromosomal instability induced by the dietary carcinogen PhIP. *Nucleic Acids Res*. 2016;44:10259–76.
- Liu X, Kramer JA, Hu Y, Schmidt JM, Jiang J, Wilson AG. Development of a high-throughput human HepG<sub>2</sub> dual luciferase assay for detection of metabolically activated hepatotoxicants and genotoxicants. *Int J Toxicol*. 2009;28:162–76.

40. Itoh T, Mitsumori K, Kawaguchi S, Sasaki YF. Genotoxic potential of quinolone antimicrobials in the in vitro comet assay and micronucleus test. *Mutat Res.* 2006;603:135–44.
41. Sobol Z, Spellman RA, Thiffeault C, Dobo KL, Schuler M. Impact of cell cycle delay on micronucleus frequency in TK6 cells. *Environ Mol Mutagen.* 2014; 55:64–9.
42. Lee SY, Kim JY, Jung YJ, Kang K. Toxicological evaluation of the topoisomerase inhibitor, etoposide, in the model animal *Caenorhabditis elegans* and 3T3-L1 normal murine cells. *Environ Toxicol.* 2017;32:1836–43.
43. Sarin N, Engel F, Kalayda GV, Mannewitz M, Cinatl J Jr, Rothweiler F, Michaelis M, Saafan H, Ritter CA, Jaehde U, Frötschl R. Cisplatin resistance in non-small cell lung cancer cells is associated with an abrogation of cisplatin-induced G2/M cell cycle arrest. *PLoS One.* 2017;12:e0181081.
44. Bhattacharya S, Das A, Datta S, Ganguli A, Chakrabarti G. Colchicine induces autophagy and senescence in lung cancer cells at clinically admissible concentration: potential use of colchicine in combination with autophagy inhibitor in cancer therapy. *Tumor Biol.* 2016;37:10653–64.
45. Blajeski AL, Phan VA, Kottke TJ, Kaufmann SH. G<sub>1</sub> and G<sub>2</sub> cell-cycle arrest following microtubule depolymerization in human breast cancer cells. *J Clin Invest.* 2002;110:91–9.
46. Trielli MO, Andreassen PR, Lacroix FB, Margolis RL. Differential Taxol-dependent arrest of transformed and nontransformed cells in the G<sub>1</sub> phase of the cell cycle, and specific-related mortality of transformed cells. *J Cell Biol.* 1996;135:689–700.
47. Michea L, Ferguson DR, Peters EM, Andrews PM, Kirby MR, Burg MB. Cell cycle delay and apoptosis are induced by high salt and urea in renal medullary cells. *Am J Physiol Renal Physiol.* 2000;278:F209–18.
48. Keyvani-Ghamsari S, Rabbani-Chadegani A, Sargolzaei J, Shahhoseini M. Effect of irinotecan on HMGB1, MMP9 expression, cell cycle, and cell growth in breast cancer (MCF-7) cells. *Tumor Biol.* 2017;39:1010428317698354.
49. Kaku Y, Tsuchiya A, Kanno T, Nishizaki T. Irinotecan induces cell cycle arrest, but not apoptosis or necrosis, in Caco-2 and CW2 colorectal cancer cell lines. *Pharmacology.* 2015;95:154–9.
50. Uen YH, Liu DZ, Weng MS, Ho YS, Lin SY. NF-kappaB pathway is involved in griseofulvin-induced G2/M arrest and apoptosis in HL-60 cells. *J Cell Biochem.* 2007;101:1165–75.
51. Katayama K, Ueno M, Yamauchi H, Nagata T, Nakayama H. K. Ethylnitrosourea induces neural progenitor cell apoptosis after S-phase accumulation in a p53-dependent manner. *Neurobiol Dis.* 2005;18:218–25.

**Ready to submit your research? Choose BMC and benefit from:**

- fast, convenient online submission
- thorough peer review by experienced researchers in your field
- rapid publication on acceptance
- support for research data, including large and complex data types
- gold Open Access which fosters wider collaboration and increased citations
- maximum visibility for your research: over 100M website views per year

**At BMC, research is always in progress.**

Learn more [biomedcentral.com/submissions](https://biomedcentral.com/submissions)

